HiSST: 2nd International Conference on
High-Speed Vehicle Science & Technology
11-15 September 2022, Bruges, Belgium

Feasibility Study of Temperature-Sensitive-Paint Technique for Use in VKI Hypersonic Facilities

Zdeněk Ilich[1], Christine Martin[2], Guillaume Grossir[3], Sébastien Paris[4], Olivier Chazot[5]

Abstract

In the present work, we aim at implementing a temperature-sensitive-paint measurement technique (TSP) for the determination of heat fluxes during experiments in the hypersonic facilities operated at the von Karman Institute for Fluid Dynamics (VKI). To do so, an evaluation method for TSP mixtures is established, including spectrometry, calibrations of paint samples under controlled conditions and benchmark tests in a hypersonic wind tunnel. At the first stage of the development, attention is paid to identify a suitable luminophore. A ruthenium-based TSP mixture is selected as a reference which undergoes the proposed evaluation methodology. The experiments performed at Mach 6 using a flat plate model confirm that the technique is as competitive as the infrared thermography. Three other luminophores are proposed for further investigation.

Keywords: *hypersonic ground testing, heat flux, TSP, flat plate*

Nomenclature

Latin

c – specific heat capacity (solid), J/kg/K
c_p – isobaric specific heat capacity, J/kg/K
h – specific enthalpy, J/kg
I – light intensity, a.u.
k – thermal conductivity, W/m/K
M – Mach number
p – pressure, Pa
$\dot{q}$ – heat flux, W/m^2
Re – Reynolds number
St – modified Stanton number
T – temperature, K
u – velocity, m/s
x – longitudinal coordinate, m
y – transverse coordinate, m

Greek

ρ – density, kg/m^3

Subscripts

0 – reservoir (stagnation)
∞ – free-stream
ref – reference
unit – per meter
w – at the wall

1. Introduction

1.1. Background

Precise characterization of the wall heat-fluxes for vehicles that experience hypersonic flow conditions is of primary importance for their survivability. Despite continuous progress in numerical tools, experi-

[1] *PhD candidate, von Karman Institute for Fluid Dynamics, Chaussée de Waterloo 72, 1640 Rhode-St-Genèse, Belgium, ilich@vki.ac.be*
[2] *STP student, von Karman Institute for Fluid Dynamics, Chaussée de Waterloo 72, 1640 Rhode-St-Genèse, Belgium, christine.martin@vki.ac.be*
[3] *Senior Research Engineer, von Karman Institute for Fluid Dynamics, Chaussée de Waterloo 72, 1640 Rhode-St-Genèse, Belgium, grossir@vki.ac.be*
[4] *Senior Research Engineer, von Karman Institute for Fluid Dynamics, Chaussée de Waterloo 72, 1640 Rhode-St-Genèse, Belgium, paris@vki.ac.be*
[5] *Professor and Head of Department, von Karman Institute for Fluid Dynamics, Chaussée de Waterloo 72, 1640 Rhode-St-Genèse, Belgium, chazot@vki.ac.be*

Copyright © 2022 by the author(s)

ments still play a significant role in this characterization. At the von Karman Institute for Fluid Dynamics in Belgium (VKI), two main low-enthalpy hypersonic facilities are operated[1]: the VKI H3 Mach 6 blow-down wind tunnel and the VKI Longshot gun tunnel (see §2).

The measurement of the wall temperature of testing articles in these facilities mostly relies on coaxial thermocouples or thin-film gauges. Although these sensors represent an accurate and reliable tool for the determination of the wall-temperature history, they are severely limited in their spatial resolution. For applications requiring a finely space resolved mapping of the wall heat flux, such as for the testing of vehicles with complex geometry or the study of boundary-layer transition, or for applications dealing with models with small internal volumes, e.g. space debris, the use of these point-wise measurements may be tedious and/or cost-inefficient. Therefore, alternative global techniques for heat-flux measurements in the VKI hypersonic facilities are of primary interest.

1.2. Global heat-flux measurements

The global techniques are typically optical measurements (the measured signal is electromagnetic radiation). Unlike point-wise measurements, a global technique can provide a map of the quantity of interest with a spatial resolution basically limited by the resolution of the optical detector.

A well-established global technique for the heat-flux measurement at VKI is infrared thermography. It has been successfully used for investigation of the boundary-layer transition in the H3 wind tunnel [1, 2, 3]. However, it is not an appropriate technique for short-duration facilities such as the Longshot. First of all, high-speed thermal imaging cameras are nowadays limited to about 1000 frames per second at a full resolution. This gives only about 20 measured points during the typical 20 ms test in the Longshot. The resulting temperature history would be too gross for reliable heat-flux determination. Also, hot particles which may be present in the free-stream can pollute the measurement as observed during previous early attempts, e.g. [4, 5].

Alternatively, strategies such as the use of thermochromic liquid crystals (TLC) and temperature sensitive paints (TSP) can provide global measurements. Although, TLC has been used in supersonic and lower-Mach hypersonic facilities [6, 7], their response time of about 3–10 ms would prove too slow for measurements in the Longshot. A wideband TLC would also require a colorized high-speed camera. Additionally, they may be sensitive to external stresses during testing that would need to be accounted for. On the other hand, the TSP technique can be a cost-effective solution that has been already successfully implemented in many hypersonic facilities, e.g. [8, 9, 10].

1.3. Fundamentals of TSP

A typical temperature-sensitive paint is made up of two primary components: a luminophore (luminescent molecule) and a polymeric, oxygen-impermeable binder. A solvent is also generally employed to facilitate the combination and dissolving of these components. If the luminophore is exposed to a light source of a specific wavelength, electrons of the luminescent molecules are excited from the ground to excited states. Upon excitation, the electrons are able to return to the ground state either through the emission of a longer wavelength light (luminescence) or through radiationless deactivation processes. The functionality of the intensity-based TSP depends entirely on the fact that with increasing temperature, the likelihood of a radiationless deactivation increases.

This effect is called thermal quenching [11]. Therefore, as the temperature of the paint increases, the intensity of its emission decreases. If calibrated, this relationship thus allows for the derivation of surface temperature and eventually of the heat flux.

1.4. Objectives

The ultimate goal of the present work is to implement the temperature-sensitive-paint technique for heat-flux measurements in the VKI Longshot hypersonic wind tunnel.

[1]Such facilities are sometimes referred to as "cold". It means that the reached total enthalpies are typically lower than during the real flight and that no high-temperature gas effects such as dissociation are present. The similarity parameters which are respected are Mach and Reynolds numbers. VKI also operates the Plasmatron as the counterpart.

Copyright © 2022 by the author(s)

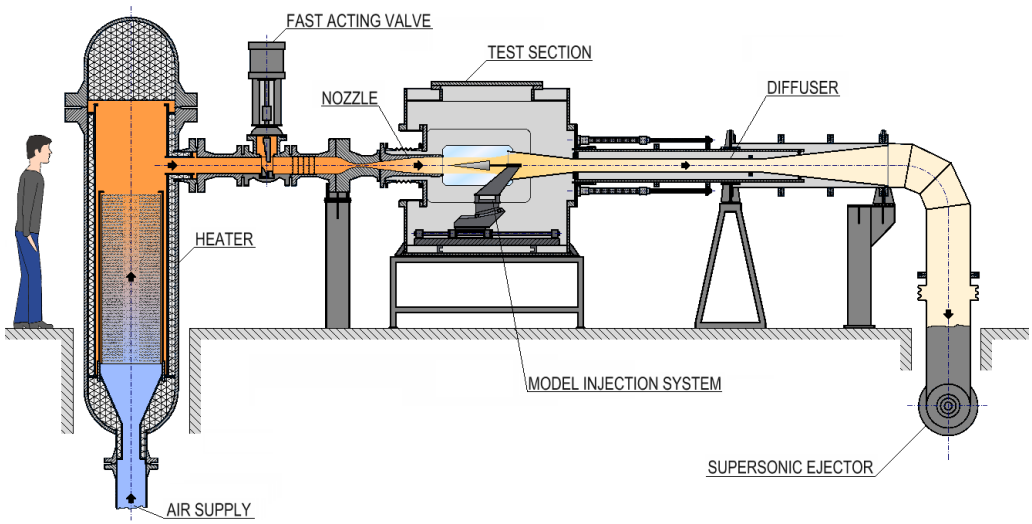

Fig 1. Sketch of the VKI H3 hypersonic wind tunnel.

To this end, a suitable TSP formula must be identified first through a multi-stage evaluation process, which is established in the present paper. It includes spectrometry, intensity-temperature calibration, and wind-tunnel benchmark testing. For the latter, the VKI H3 hypersonic wind tunnel is employed. A ruthenium-based mixture serves as a reference for verification of the methodology and for later comparison with other TSP.

This paper is organized as follows. First, the VKI low-enthalpy hypersonic facilities of interest are briefly introduced. Then, requirements for TSP imposed by the Longshot test environment are identified and listed. Besides the reference ruthenium, three other luminophores are proposed as possible candidates for future investigation. Finally, the evaluation process is presented and the performance of the reference mixture is discussed. The results obtained during the benchmark test in the H3 wind tunnel are compared to ones stemmed from previous research using infrared thermography.

2. VKI low-enthalpy hypersonic facilities

2.1. VKI H3 wind tunnel

The VKI H3 hypersonic blow-down wind tunnel is used for a variety of aerothermodynamic investigations, e.g. boundary-layer transition study [1], or study of ablation effects on aerodynamic characteristics of entry capsules [12]. The tunnel is equipped with an axisymmetric nozzle capable of producing a uniform Mach 6 free jet with a diameter of 12 cm. The VKI's main 40 bar line supplies dry air, which is heated via a pebble-bed heater prior to its expansion. The facility operates at typical stagnation pressures of $7 - 35$ bar and reaches a maximum stagnation temperature of 550 K. H3 is able to produce Reynolds numbers between $3 - 30 \times 10^6$ m^{-1}. Before testing, a supersonic ejector is employed to evacuate the test chamber. The facility features a rapid injection system that allows for the remote injection of the model once the hypersonic flow is established. Optical access is provided via two large windows, one on each side of the test chamber, as well as a single smaller window. A schematic of H3 is shown in Fig. 1.

The present TSP feasibility study is based on investigations in the VKI H3 tunnel, thanks to the long test times than can be achieved in this facility, and the numerous tests that can be run per day.

2.2. VKI Longshot wind tunnel

The VKI Longshot wind tunnel is a low-enthalpy gun tunnel, which has been operated at the von Karman Institute for Fluid Dynamics since 1967. It was designed and built by R.W. Perry and his team at the Republic Aviation Corporation (U.S.) [13]. After its installation in the VKI premises, it has been extensively used for both fundamental and applied research [14]. The Longshot has also undergone

Copyright © 2022 by the author(s)

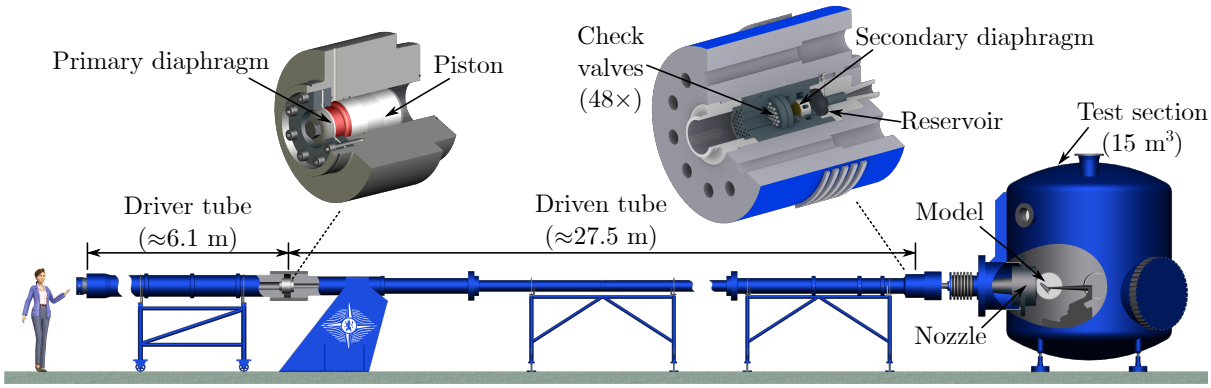

Fig 2. Sketch of the VKI Longshot hypersonic gun tunnel.

several modifications and modernizations (e.g. additions of Mach 12 and Mach 14 nozzles, automation, etc.). The sketch of the wind tunnel is given in Fig. 2 with a description of its main parts.

The Longshot wind tunnel is a world-class facility with a unique design detailed in [15] which provides an exceptionally long test time within its class (typically about 20 ms). It is a "cold" hypersonic wind tunnel specifically designed to achieve large Reynolds numbers (approx. $3 - 13 \times 10^6$ m^{-1}) at high Mach numbers (approx. $9.5 - 14$), both possibly matching flight values. The Mach-Reynolds simulation can be, therefore, ensured.

This European reference low-enthalpy hypersonic facility benefiting from a state-of-the-art free-stream flow characterization serves to validate numerical tools, to generate aerothermodynamic databases, and to investigate specific flow phenomena such as the laminar-to-turbulent transition phenomenon.

By far the most frequent test gas is nitrogen which is employed for Earth entry studies. Alternatively, CO_2 can be used as well for Martian entries. The maximum peak reservoir pressure and temperature currently achieved are on the order of 400 MPa and 2500 K, respectively. The corresponding total enthalpy is still rather low ($h_0 < 3.4$ MJ/kg) so that no dissociation effects are present providing nitrogen is used.

3. Criteria for TSP

3.1. Basic requirements for TSP

The utilization of TSP in hypersonic facilities must accommodate many specifics not present in subsonic or even supersonic testing, like high temperatures, short test time, harsh environment with possible particles in the flow, etc. Therefore, it is generally not sufficient to purchase a commercially-available TSP. Instead, the right mixture must be developed and customized to suit a particular facility.

The main evaluating criteria for the mixture can be summarized as: a suitable wavelength range of the absorption and emission spectra separated by a sufficiently large Stokes shift [11], a sufficient temperature sensitivity in the expected temperature range, a short response time (i.e. a short luminescent lifetime of the luminophore and the ability to form a thin layer since the response time is proportional to the square of the paint thickness), pressure insensitivity, and slow aging.

Since the environment in the Longshot tunnel is more challenging than the one in the H3 tunnel (shorter test time, higher stagnation temperatures, self-luminosity, the recirculation zone in the test chamber surrounding the hypersonic core, etc.), the criteria for the final TSP will be specified according to the Longshot.

3.2. Longshot specifics

One of the most important points for selection of the right luminophore is the wavelength of its absorption and emission spectra which should both lie outside any light produced by the facility itself (so-called self-luminosity). As pointed out in [16], if the self-luminosity partially overlaps with the emission spectrum, it can be directly misinterpreted as a signal from the TSP and hence erroneously lead to the lower derived

Copyright © 2022 by the author(s)

surface temperature. On the other hand, if the self-luminosity has a component in the absorption spectrum, it can additionally excite the TSP and acts as a non-uniform excitation light source.

The previous spectrometry measurements performed in the Longshot test section reveal the presence of two groups of atomic lines at 589.09 nm; 589.68 nm and 767.35 nm; 770.95 nm, which correspond to sodium and potassium, respectively. Therefore, the suitable luminophore for the Longshot should avoid these wavelengths. Furthermore, shorter wavelengths are generally preferred as there is less pollution from the radiated background. This is depicted in Fig. 3 where a more recent measurement performed by Dr. Le Quang exhibits radiation approximately corresponding to the one of a black body at 1420 K.

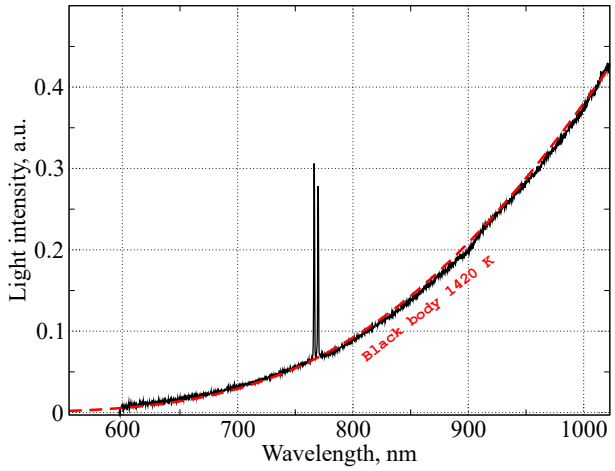

Fig 3. Spectrometry measurement in the Longshot test section. Courtesy Dr. Le Quang.

In addition to the proper excitation and emission wavelengths, it is vital that the TSP possesses a very short response time. The typical duration of a test in the Longshot is about 20 ms, thus requiring the paint to react within microseconds. The response time of the paint depends upon the luminescent lifetime of the selected luminophore, as well as the thickness of the paint itself. Ideally, this application thickness would be in the order of micrometers. However, as the paint thickness decreases, the intensity of the emissions does as well; it is important to find the proper balance between these two quantities.

Lastly, the TSP needs to be optimized for the wall temperature range typically experienced during Longshot tests. It depends on the thermal conductivity of the test article and, to a certain extent, on the specific location on it. Most of the time, either a thermally insulating material for the model or an insulating base layer must be used to ensure a sufficient rise of the surface temperature. For the foreseen applications of TSP in the Longshot, the temperatures are expected between approximately 290 K and 330 K. If the paint does not exhibit an appropriate sensitivity to the temperature within this range, the signal-to-noise ratio will be unacceptably low.

Note that besides the insulation properties, the purpose of the base layer is to provide a fine surface to which TSP itself can be applied. Also, the base layer is usually a white coat that enhances the luminescent light. Two main strategies are usually followed: the base layer can either have the same thermal properties as the TSP layer and they are both treated as a uniform medium or it has a sufficiently large thickness so that it can be treated as the semi-infinite base. In the present study, the need for a base layer is avoided by the selection of an appropriate model material (§5.2).

3.3. Considered mixtures for the initial study

During the presented initial phase, attention is paid to selecting the right luminophore although the binder markedly influences the paint performance as well. The choice of the binder along with a suitable solvent is left to a future optimization phase. A polyacrylic acid (PAA) binder dissolved in pure ethanol is considered for all mixtures hereafter.

Copyright © 2022 by the author(s)

Based on the literature review and available data sheets, four luminophores have been identified as potential candidates for investigation in the initial phase of the development. They are Ru(bpy) (tris(2,2'-bipyridyl) ruthenium), Perylene, Coumarin 153, and Rhodamine B. The TSP samples prepared for the evaluation process are depicted in Fig. 4.

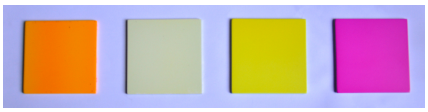

Fig 4. TSP samples. (Left to right) Ru(bpy), Perylene, Coumarin 153, Rhodamine B.

Ruthenium based TSPs have been successfully utilized by researchers at the DLR [17] and at Purdue University [18] in hypersonic applications similar to those tested in the Longshot. Therefore, the Ru(bpy) based mixture has been selected as a reference TSP throughout the development activities serving to verify the proposed evaluation process and for future comparison with other luminophores. Although Ru(bpy) is reported to have its peak theoretical absorption and emission wavelengths at about 452 nm and 620 nm, respectively [11], and hence potentially suitable for the Longshot tunnel, it is susceptible to a phenomenon referred to as "rigidochromism". As its solution dries, undergoing a phase change from liquid to solid, the manner in which the luminophore molecules interact with each other changes as well. As a result, the luminophore emits light at a shorter wavelength, creating a "blue shift" (i.e. a shift towards the blue side of the visible light spectrum) [19, 20]. This is undesirable for the Longshot since any decrease in emission wavelength would introduce the risk of self-illumination interference from the facility. Therefore, the Ru(bpy) is probably not the best choice for the Longshot facility and better alternatives remain to be identified.

4. Evaluation of TSP mixtures

The evaluation process of the TSP mixture followed in the current work consists of three basic steps. First, spectrometry is carried out for a TSP sample, preferably at several different temperatures. Then, the intensity-temperature curve is determined through calibration of a TSP sample. At last, the most promising mixtures are used for a benchmark test in the H3 wind tunnel.

The evaluation process will be applied to all considered mixtures, albeit only some of them are allowed to enter all steps based on their performance. Since the development of the TSP mixture is still ongoing, only the results for the reference Ru(bpy) based mixture are presented hereafter.

A series of high-powered LED arrays (100 W, 10×10 LED chips) cooled down by appended water heat sinks is used as the light source. For the reference ruthenium mixture, the blue LED with ($455 - 460$ nm) has been selected for the initial investigation.

4.1. Spectrometry

The spectrometry phase of the evaluation process assesses whether a mixture meets the basic requirements and refines its spectra gathered from the literature. This helps to identify an appropriate optical filter needed to isolate the TSP emission[2].

All spectrometry was performed using the OceanOptics HR4000CG-UV-NIR spectrometer coupled with a fiber patch cord (QP400-2-UV/VIS-BX).

Figure 5 shows the emission spectra of the reference Ru(bpy) mixture at several temperatures under atmospheric pressure conditions. The spectra are normalized by the peak of the excitation light (455 nm) which is also visible in the plot. The emission spectrum exhibits temperature dependency as expected. The peak emission occurs approximately at the same wavelength (about 600 nm) for the considered temperature range. The two lines of Longshot's self-luminosity at about 590 nm and 770 nm are highlighted as well. The final mixture should, however, avoid these lines.

[2]First, attention is paid to the emission characteristic when still relying on published absorption spectra. Precise measurement of the absorption spectrum for a given mixture will be performed later on during the optimization phase in order to select the most suitable light source.

Copyright © 2022 by the author(s)

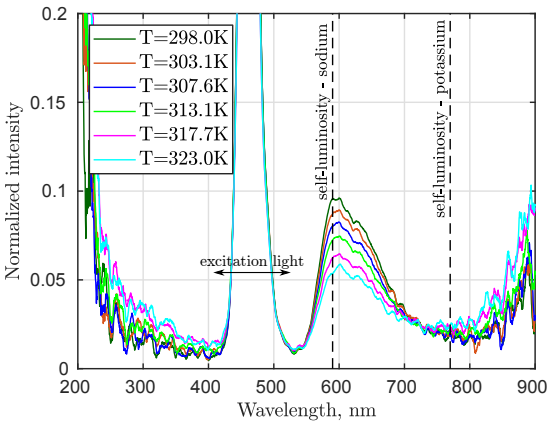

Fig 5. Emission spectra of Ru(bpy) based TSP for different temperatures.

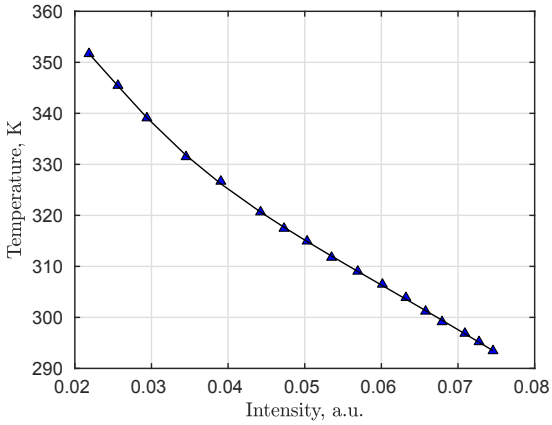

Fig 6. Intensity-temperature calibration curve of Ru(bpy) based TSP.

4.2. A priori intensity-temperature calibration

As the next step in mixture evaluation, the intensity-temperature calibration curve of the TSP mixture is measured. The calibration is carried out using a TSP sample placed in a dedicated calibration chamber (Fig. 7) where pressure and temperature can be controlled. The chamber internal volume (60 mm × 60 mm × 60 mm) is evacuated using a vacuum pump and the temperature of the sample can be changed by a Peltier cell. The sample sits on the copper base that ensures a uniform temperature field (checked a priori using an infrared technique). The temperature of the sample is monitored by a type-K thermocouple (Chromel-Alumel). The optical access for the excitation light is ensured through two side quartz windows. The emission is monitored though the top plexiglass window. As the emission is expected in the visible range the transmittance of plexiglass is assumed to be sufficient.

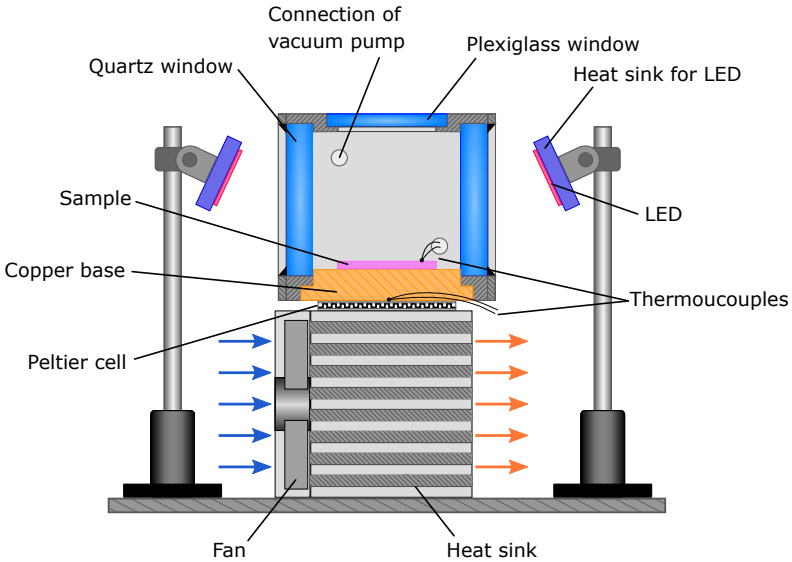

Fig 7. Calibration chamber used for a priori calibration of TSP samples.

To monitor the light intensity of emission, a high-speed black-and-white camera Phantom v710 (12-bit) which will be used for the actual testing in the H3 wind tunnel is employed. In order to account for the non-linearity of the camera chip, the correction strategy detailed in [21] is applied. The camera was placed in a dark chamber pointing to a uniform-light target. Then, a series of images were taken, each with different exposure time, and a sum of Chebyshev functions was fitted to the obtained data by the

Copyright © 2022 by the author(s)

least square method. Once the corresponding coefficients of the fit are known, they can be used to correct the camera reading both during the TSP calibration and the testing in the wind tunnel.

The same optical filter as for the actual test was placed in front of the camera lens. Since no self-luminosity is present in the H3 tunnel, the purpose of the filter is just to filter out the excitation light. Therefore, only a high-pass filter (Melles Griot 03-FCG-083) with a cut-off wavelength at about 515 nm was selected.

An example of calibration curve is presented in Fig. 6. The calibration was performed at low pressure (1.6 kPa). The temperature sensitivity is about 1.8 %/K close to room temperature. The fourth-order polynomial has been fitted to the calibrated data in terms of variables of the Arrhenius plot (i.e. $\ln(I)$ and $1/T$). The variations in the light intensity over the sample was about 4-8% (pixel-wise). Although a small contribution to the overall uncertainty is expected as the average intensity is used, the calibration setup should be further improved. Such a polynomial curve can be used to convert the light intensity to temperature. The fourth-order polynomial results in the root mean square of the residuals of 0.2 K. The combined uncertainty on temperature is 0.85 K considering 95% confidence interval. However, the real testing is expected to rely on the in-situ calibration as suggested by [8]. This will eliminate the uncertainties stemmed from different environmental conditions in the calibration chamber and during the test as well as varying properties of TSP, e.g. aging, paint thickness, etc.

The same calibration chamber was used to study the effect of aging (photodegradation of the paint in time under constant excitation) and the pressure sensitivity (due to oxygen quenching)[3]. Whereas the pressure sensitivity has been found to be negligible for the PAA binder, the aging seems to play an important role. After an hour of continuous exposition, the light intensity dropped by about 16-20%. However, the use of normalized intensity I/I_{ref} can reduce this effect.

4.3. Testing in the H3 wind tunnel

The last step of the evaluation is to perform a benchmark test in the H3 wind tunnel. The selected model is a flat plate which constitutes a favorably simple geometry and which already underwent investigation using infrared thermography by Carugno in [22]. This allows comparing both techniques directly.

A test using the reference ruthenium mixture will be presented in the next paragraph.

5. Test of ruthenium based TSP in the H3 tunnel

5.1. Setup

The test configuration and conditions were selected to closely approximate those of the infrared measurement presented in [22]. The medium Reynolds test with the nominal reservoir pressure of 20 bar was used for the comparison. Table 1 lists the main actual parameters for the present study and the infrared data [22]. Although the Reynolds number is about 14% lower for the present test, it is assumed to be close enough to allow for the qualitative comparison of both techniques.

Table 1. Summary of the test conditions.

	M	Re m^{-1}	T_0 K	p_0 bar
IR data [22]	6	1.72×10^7	515.8	22.8
Present study (at 8 s)	6	1.48×10^7	530.7	20.6

The camera and the optical setup was the same as used for the intensity-temperature calibration. The Nikon NIKKOR 50 mm objective was used with the f/2 aperture. The images were recorded in 512 × 384 resolution at 1 kHz using 25 µs of exposure time.

[3] In order to minimize the pressure sensitivity of TSP, the binder must be oxygen impermeable [11]. Since nitrogen is used as the test gas in the Longshot, this point is not so critical. However, a trace amount of oxygen can be present before a test, and the a priori calibration may be affected as well.

Copyright © 2022 by the author(s)

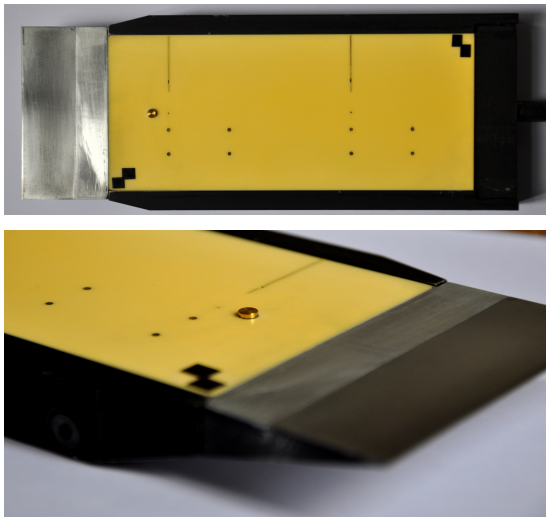

Fig 8. The flat plate model with the cylindrical roughness element and with applied TSP.

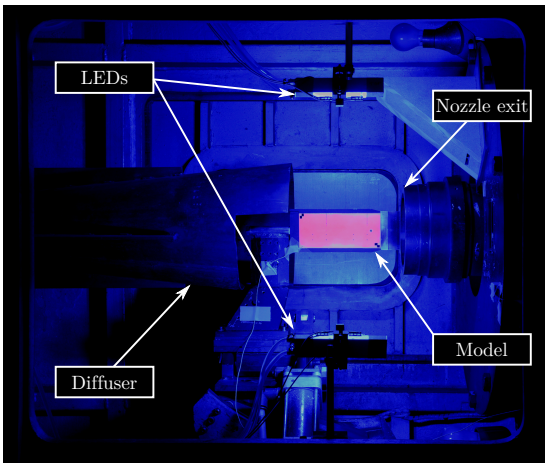

Fig 9. LEDs and model mounted in the test section of the H3 tunnel.

The tunnel conditions (the reservoir pressure and temperature, and the initial model temperature) were acquired by the H3 acquisition system (NI-6123 cards connected to terminal blocks NI TB-2709 housed in NI PXI-1036 chassis).

5.2. Model

The model selected for the benchmark test is a flat plate that features a cylindrical roughness element placed on the centerline, 60 mm from the leading edge (Fig. 8). The roughness element has a diameter of 4 mm and a height of 1 mm. The model is made of machinable glass-ceramic MACOR® material whose thermal properties are known [23]. It is also white in color, and hence perfectly suited for TSP where a highly reflective white background is needed to enhance visibility of emissions. As an insulator, it helps to increase the surface temperature rise[4].

Before testing, the central area of the model is coated with the TSP mixture in a layer of about 50 µm (estimated by the amount of the paint spent)[5]. At the same time, a 50 mm $\times$ 50 mm sample is also painted. This sample is later used to conduct the final calibration which will aid in the post-processing of test results. Small black rectangular stickers are attached to the model surface; these will aid in image alignment during post-processing. The painted model is then mounted in the test section of the H3 tunnel, such that the TSP is visible through the side window, and properly aligned (Fig. 9). The initial temperature of the model is monitored by a thermocouple attached to the surface.

5.3. Post-processing

In order to obtain the temperature field, the recorded images were post-processed using a MATLAB script as follows:

1. Ambient light frames (light-off) and reference (wind-off, light-on) frames were each averaged into a single frame.
2. Both averaged frames were corrected for camera non-linearity.
3. The average ambient light frame was subtracted from the average reference (wind-off) frame.
4. Wind-on frames were corrected for camera non-linearity.

[4]Both thermal insulation and white background are typically provided by a base coat applied on a surface before the TSP itself [11, 16]. MACOR® material eliminates the need for a base layer for the present case.

[5]The testing in the Longshot tunnel will require even thinner layer in order to be sufficiently fast.

Copyright © 2022 by the author(s)

5. The average ambient light frame was subtracted from the wind-on frames.
6. Wind-on frames were aligned with the average reference (wind-off) frame in order to account for any shifting of the model that may have taken place during testing.
7. Wind-on frames were divided by the average reference (wind-off) frame in order to calculate the intensity ratio (I/I_{ref}) for each pixel of each wind-on frame, thereby normalizing the intensity readings.
8. Calibration curve was applied to normalized intensity, resulting in the creation of a temperature field.

Once the temperature field was found for the duration of the test, they could be integrated over time to determine the corresponding heat flux. This determination was made using the method of Liu, outlined in [24], which accounts for the thin TSP layer sitting on the semi-infinite base. The thermal properties, which are assumed to be independent of temperature[6], were taken from [23] and [16] for the base material (MACOR®) and the TSP (considered to be equal to those of the PAA binder), respectively. The TSP layer was estimated to be approximately 50 µm thick.

Finally, the modified Stanton number was computed knowing the free-stream flow properties (assuming a perfect gas) as:

$$\text{St} = \frac{\dot{q}_w}{\rho_\infty u_\infty c_p (T_0 - T_w)}. \tag{1}$$

5.4. Results

The temperature field obtained on the flat-plate model is shown in Fig. 10 for three different instants of time along the course of the test. The TSP successfully indicated temperature change throughout the testing period. The increase of the surface temperature in the wake behind the cylindrical roughness element is clearly visible. The side effects on the flat plate can be observed as well.

The wall heat flux derived at 8 s after the start of the test, together with its dimensionless form (modified Stanton number), is depicted in Fig. 11[7]. Again, the symmetric hot wake downstream of the roughness element is easily noticeable. A hot zone is present in front of the blunt element due to the stagnation region and the shock wave boundary layer interaction. The performance of TSP close to neighboring surfaces (such as the side surface of the roughness) is generally weaker as discussed in the next paragraph. Therefore attention should be paid to the surface quality in these regions and to the proper interpretation of the results afterward. The wake seems to be fairly symmetric, as can be appreciated in the transversal profiles in Fig. 12.

Two vortices visible as the longitudinal strikes are formed inside the wake [27]. The latter shrinks with increasing distance from the roughness until it reaches its minimum spanwise width at a distance of about 105 mm from the leading edge (45 mm from the element center, i.e. 11.25 times the roughness width). The heat load drops accordingly. Further downstream, the spanwise expansion of the wake accompanied by increasing heat load is observed. This corresponds to the breakdown of the wake into turbulence.

As shown in Fig. 13, where streamwise profiles are plotted, the Stanton number along the model centerline starts to follow the theoretical turbulent trend at about 150 mm (90 mm from the element center, i.e. 22.5 times the roughness width).

[6] An iterative algorithm taking into account temperature dependencies of the thermal properties of materials is proposed in [25]. The case of a finite base has been investigated in [26].

[7] The derived maps are polluted by the alignment markers and by the thermocouple located in the bottom right corner. Also, the presence of previous instrumentation of the model (lines for wires, taps) is noticeable.

Copyright © 2022 by the author(s)

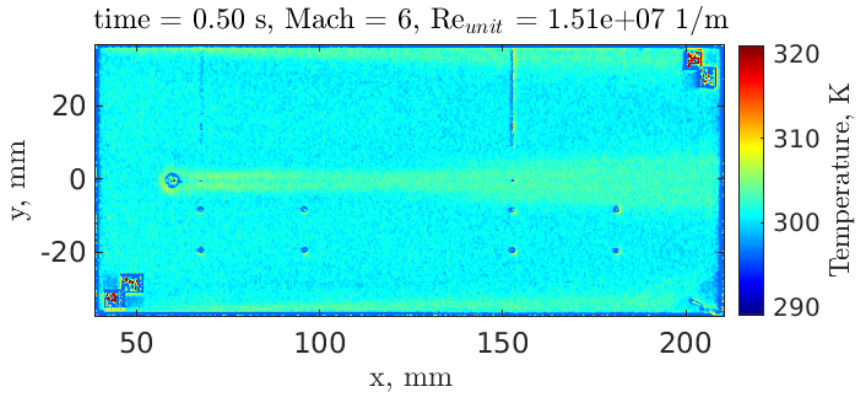

(a) Time = 0.5 s.

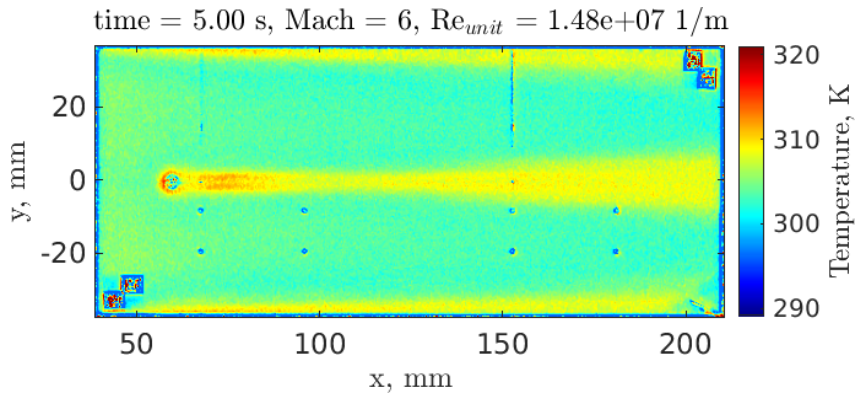

(b) Time = 5.0 s.

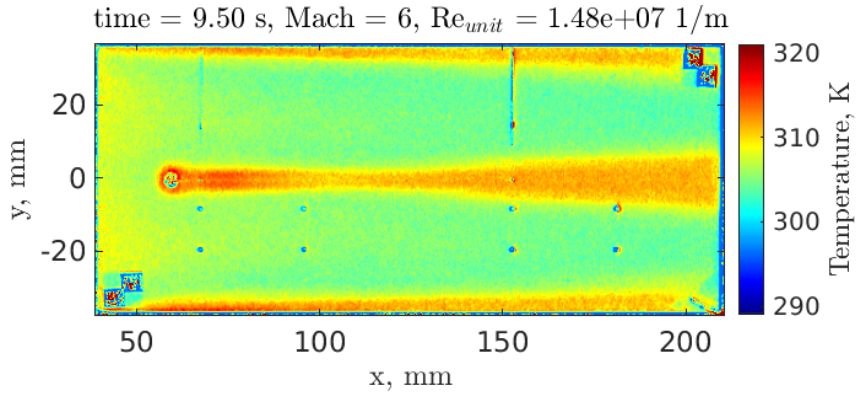

(c) Time = 9.5 s.

Fig 10. Instantaneous temperature fields at several instants of time from the test beginning. The longitudinal coordinate starts at the leading edge. Flow is from left to right.

Copyright © 2022 by the author(s)

5.5. Comparison to IR data

With respect to qualitative analysis, the generated modified Stanton number fields are consistent with the results of the infrared study conducted by Carugno in [22]. Compared to typical infrared data, the TSP measurements seem to suffer from more noise. This may be due to a lower spatial resolution of the IR camera (FLIR SC3000) and by the fact that thermal radiation is naturally more uniform than the paint.

The quality of the TSP data is compromised in the vicinity of the roughness element. This may be a result of a poor quality of the surface around the element, which suffers from multiple gluing of various roughness elements, and of the alignment process of the wind-off and wind-on frames. Also, the light reflection from the element's surface and possible shadow may worsen the situation.

It should be noted that TSP has generally a lower temperature resolution and thus some detailed features can stay imperceptible. On the opposite, a much higher spatial resolution can be achieved together with a shorter response time. The latter is of primary importance for a reliable derivation of the heat flux in short-duration hypersonic ground testing through the time integration of temperature history[8].

The experimental TSP results in terms of the modified Stanton number are quantitatively compared to Carugno's data, as well as the theoretical trends for turbulent and laminar flows computed through the reference temperature method [28]. The model was divided longitudinally into three profiles identical to those used in Carugno's analysis. The comparison of the streamwise profiles is evidenced in Fig. 13.

In the laminar region (outside the wake), both the TSP and infrared results deviate from the theoretical trend as well as from each other. The profiles exhibit a change in their trends starting at about $x = 75\,\text{mm}$ and $x = 100\,\text{mm}$ for TSP and IR data, respectively. Albeit not fully understood yet, the TSP results seem to make more sense as they agree well with the theory in the front part of the model and then the departure takes place further downstream. On the other hand, the IR results are closer to the theory towards the downstream end of the model, which is considered to be unlikely.

In the turbulent region within the wake (occurring for $x > 150\,\text{mm}$), the TSP results are consistent with the theoretical trend. However, they are slightly offset from the previously obtained infrared results. Namely, the profiles start to follow the theoretical turbulent trend about 25 mm further downstream than the IR data. This can be partially caused by the lower Reynolds number achieved for the present test.

As already mentioned, the TSP profiles carry more noise than IR data, although it can be a result of different data processing to a certain extent. Note that for areas with different backgrounds (e.g. the spots from previous instrumentation), the TSP is not able to provide reliable data. For these locations, IR results are less corrupted as the body still radiates despite different emissivity.

5.6. Uncertainty quantification

The final uncertainty in the derived heat flux remains to be determined once the right luminophore is identified and the TSP mixture is optimized (appropriate binder, concentration, layer thickness, light source). Using an a priory calibration, researches in DLR claim an overall uncertainty of 16% in the heat flux for conditions relatively similar to the those in the Longshot [16].

For the present study, various sources of uncertainty have been identified as: the thickness of the TSP layer, thermal properties of TSP and the base, temperature-intensity calibration, and additional sources (camera non-linearity correction, aging, chemical stability, and pressure sensitivity).

Although the thickness of the TSP layer is expected to have a limited effect (as also demonstrated in [16]), it is hard to be precisely measured and controlled. Therefore, a large uncertainty of 50% is assumed on this quantity. The measurements of the thermal properties of the materials involved are also intricate. Being very thin, the thermal properties of the TSP layer itself can be negligible. The properties of the based (MACOR®) were taken from the fits presented in [23]. Unfortunately, it was

[8]The time integration is also a process that naturally amplifies the signal noise.

Copyright © 2022 by the author(s)

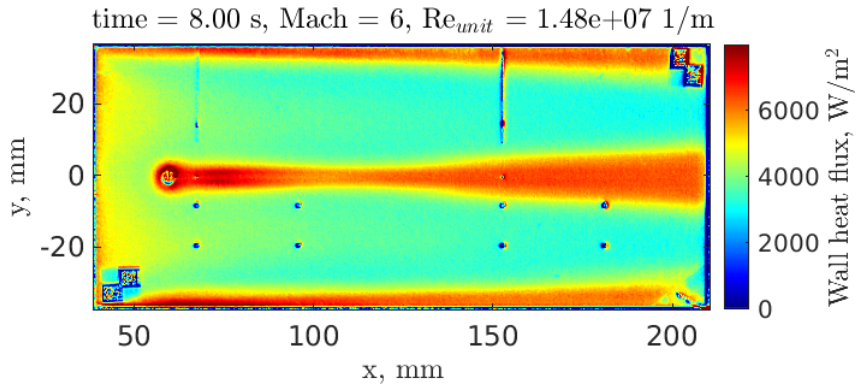

(a) Heat flux.

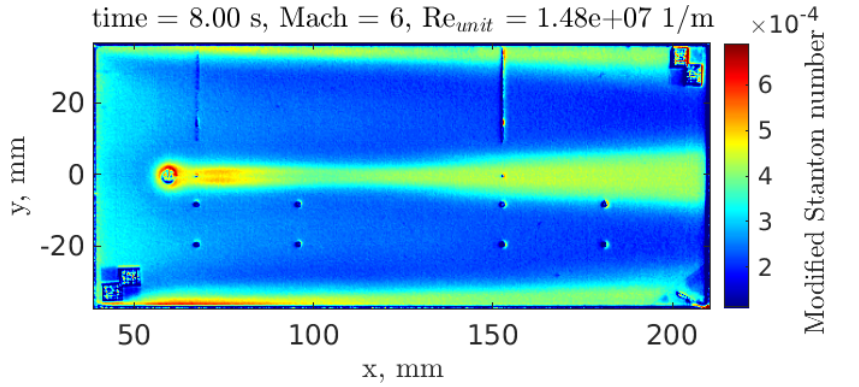

(b) Modified Stanton number (see eq. 1).

Fig 11. Derived quantities at time = 8 s. The longitudinal coordinate starts at the leading edge. Flow is from left to right.

not possible to quantify the uncertainties on each parameter. Instead, the uncertainty of 15% on the thermal product (ρck) was hypothesized as a typical value achievable by experimental measurement of this quantity. The uncertainty of temperature resulting from the a priory calibration is 0.3%. An additional contribution of 5% to the overall uncertainty in the heat flux is assumed from the additional sources. Considering these uncertainties in the input quantities, the overall uncertainty in the derived heat flux is estimated to be about 9%.

This coarse estimation is significantly lower than one from [16]. A proper uncertainty quantification using one of the various sampling-based approaches (e.g. Latin hypercube sampling (LHS) using the DAKOTA code [29]) may reduce/decrease the value. In order to reduce the uncertainty, an in-situ calibration employing an embedded coaxial thermocouple can be alternatively used [8].

6. Conclusions

The methodology for the preparation and application of TSP customized for the VKI hypersonic facilities has been established. The evaluation procedure for assessment of TSP performance along with all needed accessories has been designed. The reference ruthenium-based mixture underwent the evaluation including the benchmark test in the H3 hypersonic wind tunnel. The obtained results reveal that TSP can be as competitive as the infrared thermography. Although it usually provides a lower temperature resolution, it still offers a much higher sampling rate and higher spatial resolution.

Copyright © 2022 by the author(s)

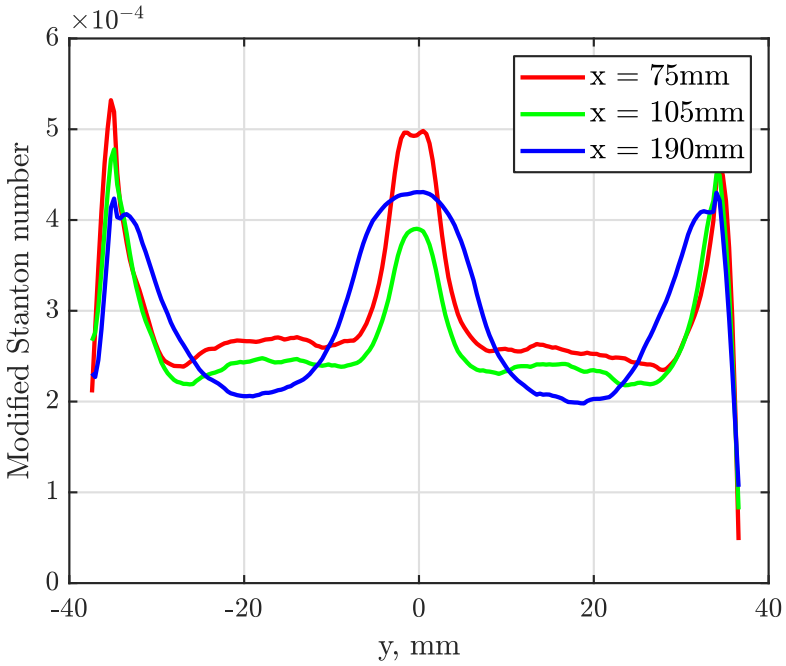

Fig 12. Transversal profiles of modified Stanton number.

The need for an in-situ calibration is foreseen for the actual testing using the TSP technique. However, it is not considered as a drawback with respect to the infrared thermography since the latter usually requires a similar approach due to unknown values of object emissivity and environment transmissivity.

Three other luminophores have been proposed for further investigation. Preliminary results show that Coumarin 153 is among the most promising ones.

In the future, the presented methodology should allow selecting and optimizing the TSP mixture for the VKI Longshot wind tunnel.

Acknowledgments

The authors wish to thank Dr. Le Quang for his help concerning the spectrometry and the optical setup.

References

[1] D. Masutti. *Ground testing investigation of hypersonic transition phenomenon for a re-entry vehicle*. PhD thesis, von Karman Institute for Fluid Dynamics - Technische Universiteit Delft, 2013.

[2] P. Dehairs. Interaction of ablation pyrolysis gases with the boundary layer in hypersonic regime. PR 2016-08, von Karman Institute for Fluid Dynamics, June 2016.

[3] N. Martin. Flight induced distributed roughness effects on boundary layer transition at mach 6. PR 2018-20, von Karman Institute for Fluid Dynamics, June 2018.

[4] H. Bottini. EXPERT-vehicle aerothermodynamic investigation. PR 2006-05, von Karman Institute for Fluid Dynamics, 2006.

[5] A. Wagner. Investigation on roughness induced transition in the VKI Longshot facility. Project report 2008-29, von Karman Institute for Fluid Dynamics, June 2008.

[6] H. Babinsky and J. A. Edwards. Automatic liquid crystal thermography for transient heat transfer measurements in hypersonic flow. *Experiments in Fluids*, 21(4):227–236, August 1996.

Copyright © 2022 by the author(s)

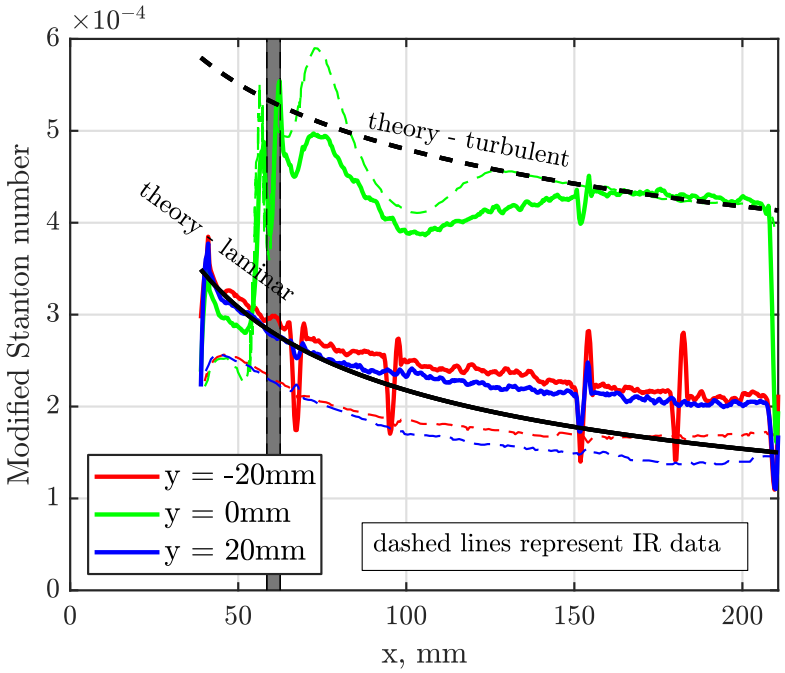

Fig 13. Longitudinal profiles of modified Stanton number. Comparison between TSP, infrared thermography [22], and theory [28].

[7] D. J. Mee, H. S. Chiu, and P. T. Ireland. Techniques for detailed heat transfer measurements in cold supersonic blowdown tunnels using thermochromic liqui crystals. *International Journal of Heat and Mass Transfer*, 45:3287–3297, 2002.

[8] S. J. Laurence, H. Ozawa, J. Martinez Schramm, C. S. Butler, and K. Hannemann. Heat-flux measurements on a hypersonic inlet ramp using fast-response temperature-sensitive paint. *Experiments in Fluids*, 60(4):70, Mar 2019.

[9] V. Borovoy, V. Mosharov, A. Noev, and V. Radchenko. Temperature sensitive paint application for investigation of boundary layer transition in short-duration wind tunnels. In *EUCASS Proceedings Series - Advances in AeroSpace Sciences*, volume 3, pages 15–24, 2012.

[10] M. Taguchi, R. Maruyama, T. Sato, and K. Mori. Measurements by temperature sensitive paint on flexible and deforming model in hypersonic flow. *TRANSACTIONS OF THE JAPAN SOCIETY FOR AERONAUTICAL AND SPACE SCIENCES, AEROSPACE TECHNOLOGY JAPAN*, 14(ists30):Pe_63–Pe_69, 2016.

[11] T. Liu and J. P. Sullivan. *Pressure and Temperature Sensitive Paints*. Springer-Verlag Berlin Heidelberg, 2005.

[12] A. Turchi, S. Paris, P. W. Agostinelli, F. Grigat, S. Lohle, D. Bianchi, and L. Ferracina. Assessment of the effect of heat-shield ablation on the aerodynamic performance of re-entry capsules in hypersonic flows. In *8th European Conference for Aeronautics and Space Sciences (EUCASS)*, 2019.

[13] R. W. Perry. The Longshot type of high-Reynolds number hypersonic tunnel. In *Third hypervelocity techniques symposium*, Advanced experimental techniques for study of hypervelocity flight, March 1964.

[14] G. Simeonides. The VKI hypersonic wind tunnels and associated measurement techniques. Technical Memorandum 46, von Karman Institute for Fluid Dynamics, November 1990.

Copyright © 2022 by the author(s)

[15] G. Grossir. *Longshot hypersonic wind tunnel flow characterization and boundary layer stability investigations*. PhD thesis, von Karman Institute for Fluid Dynamics - Université Libre de Bruxelles, July 2015.

[16] H. Ozawa, S. J. Laurence, J. Martinez Schramm, A. Wagner, and K. Hannemann. Fast-response temperature-sensitive-paint measurements on a hypersonic transition cone. *Experiments in Fluids*, 56(1853):1–13, 2015.

[17] J. Martinez Schramm, K. Hannemann, H. Ozawa, W. Beck, and C. Klein. Development of temperature sensitive paints in the high enthalpy shock tunnel Göttingen, HEG. In *8th European Symposium on Aerothermodynamics for Space Vehicles*, Lisbon, 3 2015.

[18] C. A. C. Ward, B. M. Wheaton, A. Chou, P. L. Gilbert, L. E. Steen, and S. P. Schneider. Boundary-layer transition measurements in a Mach-6 quiet tunnel. In *40th AIAA Fluid Dynamics Conference and Exhibit*, number AIAA paper 2010-4721, 2010.

[19] W. R. Glomm, S. Volden, J. Sjöblom, and M. Lindgren. Photophysical properties of ruthenium(II) tris(2,2`-bipyridine) and europium(III) hexahydrate salts assembled into sol−gel materials. *Chemistry of Materials*, 17(22):5512–5520, November 2005.

[20] E. L. Sciuto, M. F. Santangelo, G. Villaggio, F. Sinatra, C. Bongiorno, G. Nicotra, and S. Libertino. Photo-physical characterization of fluorophore ru(bpy)32+ for optical biosensing applications. *Sensing and Bio-Sensing Research*, 6:67 – 71, 2015.

[21] H. F. Leite, H. Sakaue, A. C. Avelar, and R. G. Silva. *Identifying and Correcting Optical and Camera Error Sources in Fast-PSP Experiments*. 2019.

[22] P. Carugno. Quantitative infrared measurements for heat-flux determination in hypersonic regime. SR 2012-37, von Karman Institute for Fluid Dynamics, Rhode-St-Genese, Belgium, 2013.

[23] B. R. Hollis. User's manual for the one-dimensional hypersonic experimental aero-thermodynamic (1dheat) data reduction code. Technical Report 4691, NASA, 1995.

[24] T. Liu, Z. Cai, J. Lai, J. Rubal, and J. P. Sullivan. Analytical method for determining heat flux from temperature-sensitive-paint measurements in hypersonic tunnels. *Journal of Thermophysics and Heat Transfer*, 24(1):85–94, January 2010.

[25] Z. Cai, T. Liu, B. Wang, J. Rubal, and J. P. Sullivan. Numerical inverse heat transfer analysis for temperature-sensitive-paint measurements in hypersonic tunnels. *Journal of Thermophysics and Heat Transfer*, 25(1):59–67, 2011.

[26] T. Liu, J. Montefort, S. Stanfield, S. Palluconi, J. Crafton, and Z. Cai. Analytical inverse heat transfer method for temperature-sensitive-coating measurement on a finite base. *International Journal of Heat and Mass Transfer*, 118:651 – 662, 2018.

[27] S. C. Tirtey, O. Chazot, and L. Walpot. Characterization of hypersonic roughness-induced boundary layer transition. *Experiments in Fluids*, 50(2):407–418, February 2011.

[28] E. R. G. Eckert. Engineering relations for heat transfer and friction in high-velocity laminar and turbulent boundary-layer flow over surfaces with constant pressure and temperature. *Transactions of the ASME*, 78(6):1723–1283, August 1956.

[29] B. M. Adams, M. S. Ebeida, M. S. Eldred, J. D. Jakeman, L. P. Swiler, J. A. Stephens, D. M. Vigil, T. M. Wildey, W. J. Bohnhoff, K. R. Dalbey, J. P. Eddy, R. W. Hooper, K. T. Hu, L. E. Bauman, P. D. Hough, and A. Rushdi. Dakota, a multilevel parallel object-oriented framework for design optimization, parameter estimation, uncertainty quantification, and sensitivity analysis: Version 6.3 user's manual. Technical Report SAND2014-4633, Sandia, July 2014.

Copyright © 2022 by the author(s)